



## Binding Interactions of TMAP to Triple- and Double Helical DNA

Nanjung Kim, Sangheon Yoo and Sungho Huh\*

Department of Biochemistry, Chungnam National University

Daejeon, Korea 305-764

Received September 21, 2006

**Abstract** : Binding interactions between a positively charged porphyrin derivative TMAP(meso-tetra(p-trimethylanilinium-4-yl)porphyrin) and triple helical (dT)<sub>12</sub>·(dA)<sub>12</sub>·(dT)<sub>12</sub>, as well as double helical (dA)<sub>12</sub>·(dT)<sub>12</sub> have been studied with NMR, UV and CD spectroscopy to obtain the detailed information about the binding mode and binding site. UV melting studies showed both DNA duplex and triple helix represented very similar UV absorption patterns upon binding TMAP, but the presence of third strand of triple helical (dT)<sub>12</sub>·(dA)<sub>12</sub>·(dT)<sub>12</sub>, inhibited improvement in thermal stability in terms of melting temperature, T<sub>m</sub>. In addition, the TMAP molecule is thought to bind to the major groove, according to CD and NMR data. But absence of the clear isosbestic point in UV absorption spectra represented that binding of TMAP to DNA duplex as well as DNA triplex did not show a single binding mode, rather complex binding modes.

Key words : cationic porphyrin, DNA, binding, stability, NMR, UV, CD

### INTRODUCTION

Positively charged water soluble porphyrin derivatives have been considered to be important in antitumor chemotherapy, mainly because of their ability to make complexes with and cleave DNA phosphodiester bonds, as described in works by Fiel et al.<sup>1</sup>. Since the molecular recognition and specific interaction of DNA is of fundamental to the biological role of DNA, the analysis of the interactions of ligands with DNA continues to be an important area in the life science. Within the context of this interest, binding of porphyrin derivatives to DNA is of considerable interest. Cationic porphyrins containing four pyrole

\*To whom correspondence should be addressed. E-mail : sungho@cnu.ac.kr

rings and conjugated double bonds have also been reported to be able to interact with DNA and cause cleavage of DNA phosphodiester bonds with the aid of irradiation of UV light.<sup>2-5</sup> They show various interacting patterns in binding to DNA, depending on the followings: (i) the number and position of positive charges, (ii) the position, the type, and the number of substituents at the porphyrin ring and (iii) the base sequence of DNA. Presence or absence and the type of the coordinated metal ion show also an important effect on the binding pattern. Based on the facts, all of Coulombic, hydrophobic, and steric interactions might be involved in binding of porphyrin to DNA. The favorable sites for intercalation and groove binding of cationic porphyrin to DNA have been reported to be 5'-CG-3' and 5'-AT-3', respectively.<sup>6-9</sup> Thus *meso*-tetrakis-(4-*N*-methylpyridiniumyl)porphyrin(T4MPyP), Cu(II)T4MPyP and Ni(II)T4MPyP are reported to bind to 5'-CG-3' sites, but *meso*-tetrakis-(2-*N*-methylpyridiniumyl)porphyrin(T2MPyP), Zn(II)TMPyP, Fe(III)T4MPyP, and Co(III)T4MPyP do not. Intercalation of T4MPyP occurs at 5'-CG-3' sites of poly(dG-dC), but T4MPyP is also able to bind to 5'-AT-3' sites of poly(dA-dT) in the groove or in the manner of outside stacking along the phosphate backbone chain. According to the X-ray crystallographic studies, Cu(II)T4MPyP hemiintercalated at the 5'-CG-3' steps of d(CGATCG)<sub>2</sub>, but Ni(II)T4MPyP did not intercalate into d(CCTAGG)<sub>2</sub>. Instead, Ni(II)T4MPyP stacked onto the ends of d(CC TAGG)<sub>2</sub>. On the other hand, stacking of T4MPyP in the major groove of both the d(A)<sub>12</sub>-d(T)<sub>12</sub> and the d(G)<sub>12</sub>-d(C)<sub>12</sub> duplexes based on the CD studies.<sup>10</sup> Here we present NMR and spectroscopic results on the interaction of *meso*-tetra(*p*-trimethylanilinium-4-yl)porphyrin(TMAP) with DNA duplex and triplex (Fig. 1).

## MATERIAL AND METHODS

### *Sample Preparation*

The model DNA oligomers triple helical (dT)<sub>12</sub>·(dA)<sub>12</sub>·(dT)<sub>12</sub> and double helical (dA)<sub>12</sub>·(dT)<sub>12</sub> were synthesized with a DNA synthesizer (ABI 391 PCR MATE) by β-cyanoethylphosphoramidite chemistry in solid phase. They were purified by using dialysis tubing with molecular weight cutoff range of 2,000 and passing through a Chelex100

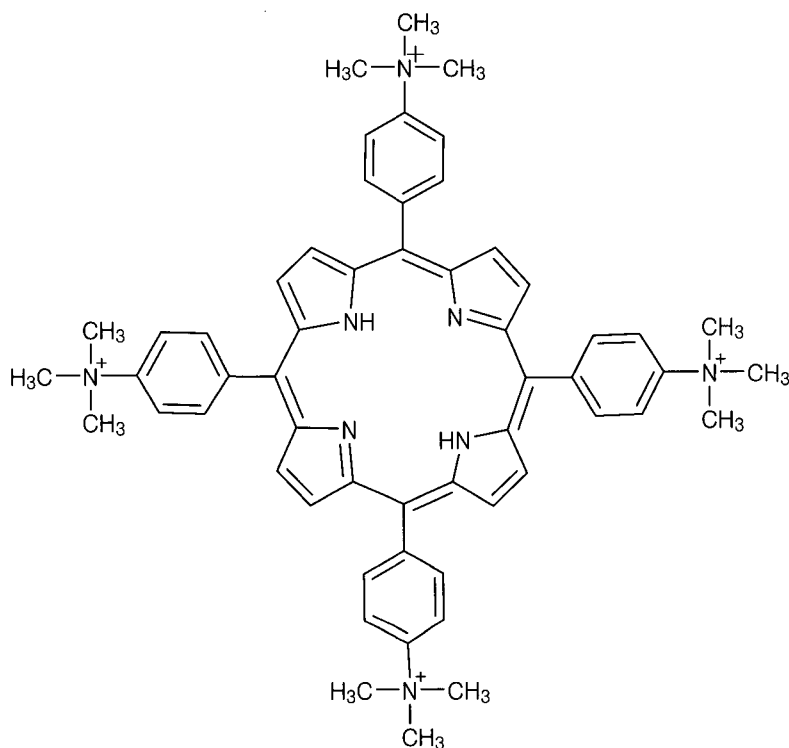


Fig. 1. The chemical structure of of *meso*-tetrakis(para-N-trimethylamminium) porphine (TMAP)

column to remove heavy metal ions and then lyophilized. DNA concentration was calculated by measuring its absorbance at 260 nm with an extinction coefficient  $\epsilon_{260} = 1.15 \times 10^5 \text{ M}^{-1} \text{ cm}^{-1}$ . All sample solutions were prepared in 20mM sodium phosphate buffer (pH 6.92) containing 100 mM NaCl.

The cationic porphyrins of *meso*-tetrakis(para-N-trimethylamminium)porphine tetra-*p*-tosylate salt(TMAP; Fig. 1) was purchased from Sigma Aldrich Chemical Co. and were used without further purification. Concentrations of the TMAP were calculated spectrophotometrically by measuring their absorbances at the Soret band with extinction coefficients  $\epsilon_{412} = 4.16 \times 10^5 \text{ M}^{-1} \text{ cm}^{-1}$ (TMAP)<sup>18</sup>. Porphyrin solutions were prepared in the same way as for DNA for all the experiments.

### ***UV and Circular Dichroism(CD) spectroscopy***

UV experiments were carried out with a HP8452A UV-VIS spectrophotometer equipped with a Peltier temperature controller. The melting experiments were performed by monitoring UV absorbance at 260nm from 10 °C to 80 °C. Melting experiments with the complex between DNA and equimolar concentration of each porphyrin derivatives were also performed in the same method as described above. UV absorption spectral changes of TMAP upon titrating with aliquots of triple helical (dT)<sub>12</sub>·(dA)<sub>12</sub>·(dT)<sub>12</sub> and double helical (dA)<sub>12</sub>·(dT)<sub>12</sub> were monitored in the range of 350-500 nm as a function of *r*, the ratio of molar concentration of TMAP to that of triple or double helical DNA. Circular dichroism spectra were obtained on a JASCO J-600 circular dichroism spectropolarimeter. The spectropolarimeter was calibrated with aqueous 0.06 % NH<sub>4</sub>-CSA solution. The regions of 220-320 and 400-500 nm were used to monitor the DNA region and the porphyrin Soret band, respectively.

### ***NMR Spectroscopy***

All NMR experiments were performed on a Unity Inova 400 spectrometer (Varian Associates, U.S.A.) with a 9.4 Tesla superconducting magnet in Central Research Facilities of Chungnam National University. Water signal suppression was achieved with the WATERGATE (Water suppression by gradient-tailored excitation) as well as presaturation pulse sequence. Chemical shifts of <sup>1</sup>H spectra were reported in ppm relative to the methyl resonance of internal 2, 2-dimethyl-2-silapentane-5-sulfonic acid (DSS) at 0.0 ppm. To observe labile proton signals, the sample was dissolved in aqueous 20 mM sodium phosphate buffer with 20% D<sub>2</sub>O (pH 6.92), containing 100 mM NaCl. The titrations of DNA oligomer with TMAP were carried out at 20°C. To observe nonlabile proton resonances, DNA sample was dissolved in 20 mM sodium phosphate buffer (pH 6.92) with 99.99 % D<sub>2</sub>O, containing 100 mM NaCl. <sup>1</sup>H NMR spectra of porphyrin-DNA complexes were recorded as the same way described above.

Table 1. Melting temperature( $T_m$ ) of TMAP-double helical  $(dA)_{12} \cdot (dT)_{12}$ , and TMAP-triple helical  $(dA)_{12} \cdot 2(dT)_{12}$ .

	$T_m$ of Double helical $(dA)_{12} \cdot (dT)_{12}$	$T_m$ of Triple helical $(dA)_{12} \cdot 2(dT)_{12}$
Free DNA	$22 \pm 2$ °C	$32 \pm 2(17 \pm 2)$ °C
DNA:TMAP = (1:1) complex	$37 \pm 2$ °C	$35 \pm 2(13 \pm 2)$ °C
DNA:TMAP = (1:2) complex	$41 \pm 2$ °C	$35 \pm 2(13 \pm 2)$ °C

\* Values in ( ) represent melting temperature of Hoogsteen pairing.

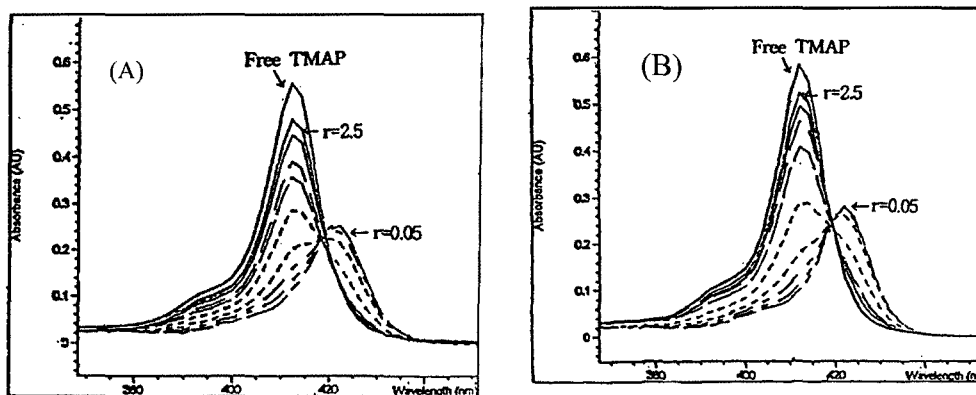


Fig. 2. UV spectral changes of TMAP upon binding to triple helical  $(dA)_{12} \cdot 2(dT)_{12}$ (upper) and double helical  $(dA)_{12} \cdot (dT)_{12}$ (lower). Values of  $r$  are 2.5, 1.25, 1.0, 0.5, 0.25, 0.17, 0.10, and 0.05.

## RESULTS AND DISCUSSIONS

### *Effect of binding of TMAP to triple helical (dT)<sub>12</sub>·(dA)<sub>12</sub>·(dT)<sub>12</sub> and double helical (dA)<sub>12</sub>·(dT)<sub>12</sub> on thermal stability*

According to the melting data shown in Table 1, binding of TMAP to triple helical DNA caused a slight increase in melting temperature of Watson-Crick pairing by 3 °C, but caused a slight decrease in melting temperature of Hoogsteen pairing by 4 °C. This meant that TMAP binding did not affect the thermal stability of the triple helical DNA significantly. In contrast, TMAP binding to double helical (dA)<sub>12</sub>·(dT)<sub>12</sub> caused a considerable increase in the melting temperature, from 22 °C to 37 °C. From these results it became clear that the presence of the third strand (dT)<sub>12</sub> in the major groove of triple helical (dT)<sub>12</sub>·(dA)<sub>12</sub>·(dT)<sub>12</sub> inhibits stabilization of the DNA double helix when TMAP binds to DNA. Therefore TMAP is considered to bind a double helical (dA)<sub>12</sub>·(dT)<sub>12</sub> at or near the major groove. This is well agreed with a result reported previously.<sup>10</sup>

### *Changes in UV absorption spectra by interactions of TMAP to triple helical (dT)<sub>12</sub>·(dA)<sub>12</sub>·(dT)<sub>12</sub> and double helical (dA)<sub>12</sub>·(dT)<sub>12</sub>*

UV absorption spectral changes of TMAP were observed in the range of 350-500 nm as a function of the ratio of molar concentration of TMAP to that of triple or double helical DNA (Fig. 2 A, B). The intensities of the Soret bands at 412 nm decreased gradually upon complexation with DNA and began to increase from the *r* values lower than 0.17. At the same time the Soret band showed a red shift from *r* values lower than 0.17. The Soret band appeared at 423 nm and showed about 50 % of hypochromicity at *r* value of 0.05, for both triple and double helical DNA. In the experiment, it can be regarded that the spectral changes upon addition of DNA to TMAP are caused by binding interaction of TMAP with DNA, therefore the spectral changes allow quantitation of DNA-TMAP binding. Absence of the clear isosbestic point indicated no simple equilibrium between free and bound TMAP at the single binding site, but the multiple binding modes or sites. And the significant hypochromicity might be due to stacking of TMAP along the DNA helix and perturbation of  $\pi$  electrons of TMAP by interaction with DNA.

### ***Induced Circular Dichroism upon binding of TMAP to DNA***

Both triple and double helical DNA showed clear induced CD spectra in the range of 350-450 nm. The induced CD for the complex of TMAP-DNA duplex showed positively induced peaks at 410 nm, indicating the surface binding mode of TMAP<sup>6</sup>. But induced CD signals also shown somewhat conservative characteristics at  $r$  of larger than 0.2, therefore TMAP might bind additionally to DNA samples in the self-stacking mode (Fig. 3 A, B)<sup>6</sup>. For triple helical  $(dT)_{12} \cdot (dA)_{12} \cdot (dT)_{12}$ , TMAP binding caused more conservative induced CD, indicating self-stacking is predominant over surface binding which was shown in the induced CD for the double helical  $(dA)_{12} \cdot (dT)_{12}$ .

### ***Imino proton resonance signals of triple- and double helical DNA-TMAP complexes***

Binding of TMAP caused increase in the linewidth of resonance signals of both DNAs. Imino resonance signals from the Hoogsteen pairing also disappeared at the  $r$  value of about 0.10. Destabilization for a double helical  $(dA)_{12} \cdot (dT)_{12}$ , was more significant than that for a triple helical  $(dT)_{12} \cdot (dA)_{12} \cdot (dT)_{12}$  (Fig. 4). This might be due to increase in the exchange rate upon binding of TMAP to DNA, and TMAP considered to bind to the double helical DNA,  $(dA)_{12} \cdot (dT)_{12}$  more properly than to the triple helical DNA  $(dT)_{12} \cdot (dA)_{12} \cdot (dT)_{12}$ . This also represented that TMAP might position at near the major groove of the DNA duplex.

### ***Phenyl proton signals of TMAP showed downfield chemical shifts upon binding to DNA***

The phenyl protons of TMAP showed downfield chemical shift upon binding. Phenyl protons at 2, 6 and 3, 5 positions showed 0.22, and 0.5 ppm downfield shift, respectively (Table 2). This could be due to rotation of the substituent group from the vertical arrangement against the porphyrin ring plane into the arrangement of the phenyl group with lower angle than vertical arrangement, upon binding.

### ***Two-dimensional NOESY spectra of DNA-TMAP complexes***

TMAP binding to a double helical  $(dA)_{12} \cdot (dT)_{12}$  caused disappearance of NOE between NH of thymine base at position 4 and H2 of adenine base at position 5 (Fig. 5). The NOE connectivity between H8 of adenine base and the imino proton of thymine base of the third strand became weak more readily than Watson-Crick paired imino protons with increase of

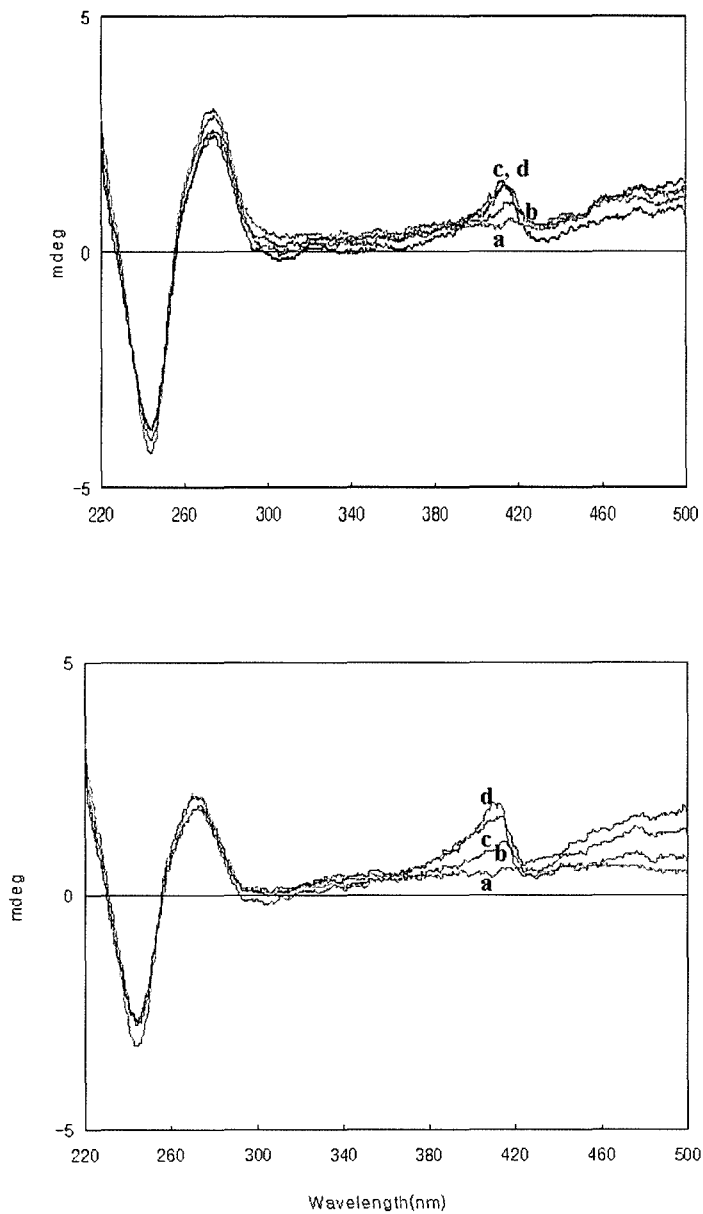


Fig. 3. CD spectra of TMAP-triple helical  $(dA)_{12} \cdot 2(dT)_{12}$ (upper) and TMAP-double helical  $(dA)_{12} \cdot (dT)_{12}$  complex(lower). (a)  $r=0$ , (b)  $r=0.1$ , (c)  $r=0.2$ , (d)  $r=0.3$ .



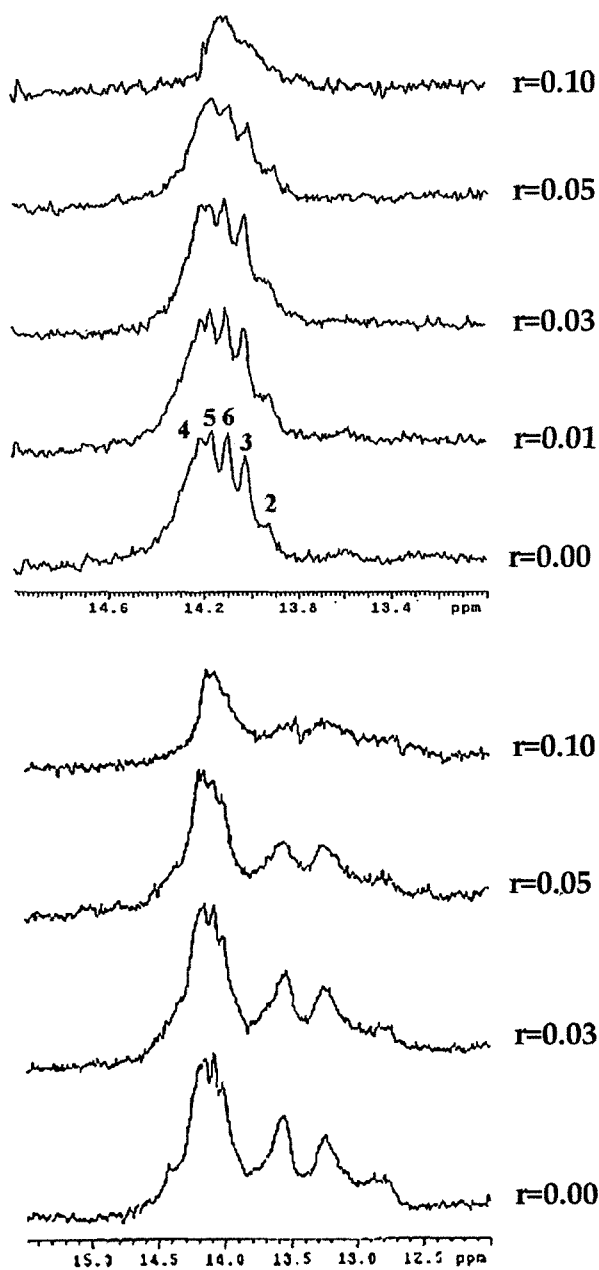


Fig. 4. Imino proton signals of double helical  $(dA)_{12} \cdot (dT)_{12}$  and triple helical  $(dA)_{12} \cdot 2(dT)_{12}$  upon binding to TMAP at various  $r$  values.

Table 2. Chemical shifts of 2,6 and 3,5 protons of the phenyl group of TMAP, TMAP-double helical (dA)<sub>12</sub>·(dT)<sub>12</sub>, and TMAP-triple helical (dA)<sub>12</sub>·2(dT)<sub>12</sub>.

Proton positions	Free TMAP	Duplex-TMAP	Triplex-TMAP
2, 6	8.04 ppm	8.26 ppm	8.24 ppm
3, 5	7.90 ppm	8.40 ppm	8.38 ppm

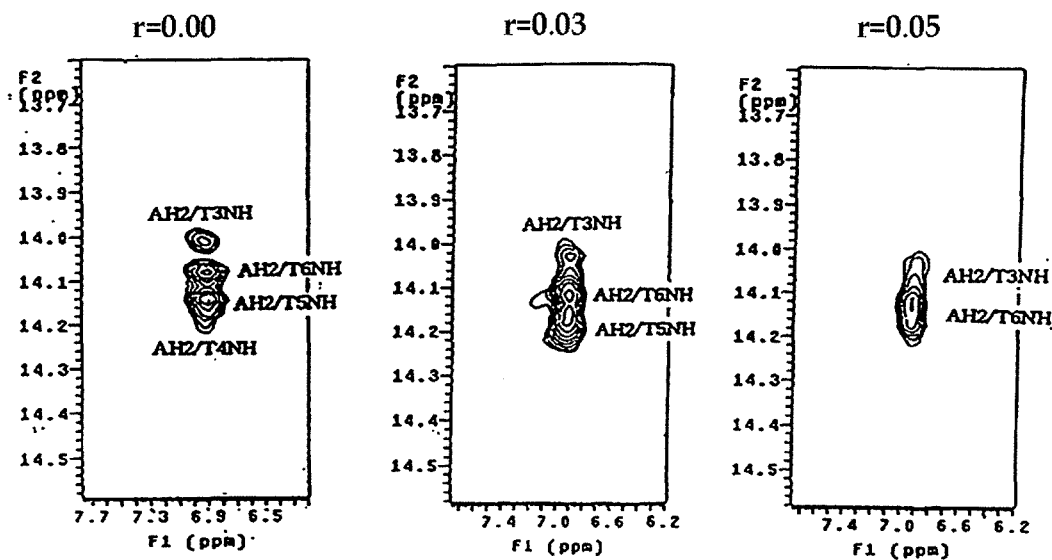


Fig. 5. 2D NOE signals between imino protons and base protons of TMAP-double helical (dA)<sub>12</sub>·(dT)<sub>12</sub> complex at different  $r$  values.

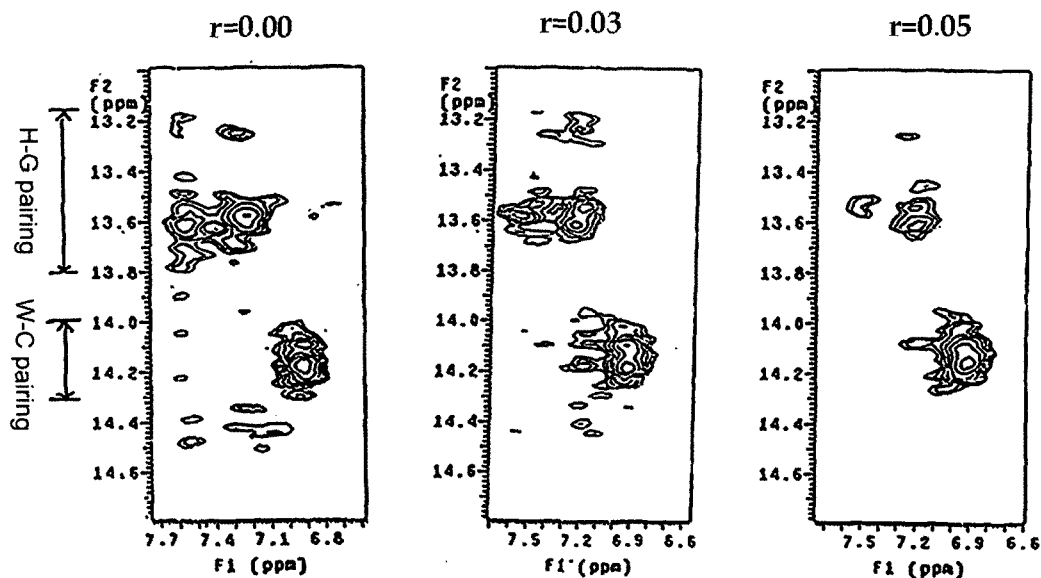


Fig. 6. 2D NOE signals between imino protons and base protons of TMAP-triple helical  $(dA)_{12} \cdot 2(dT)_{12}$  complex at different  $r$  values.

[TMAP]/[DNA] ratio for the triple helical DNA  $(dT)_{12} \cdot (dA)_{12} \cdot (dT)_{12}$ . (Fig. 6).

### <sup>31</sup>P-NMR experiments

The structural deformation of the major backbone of DNA caused by interaction with TMAP is considered to involve C5'-O5' torsional angle.<sup>11</sup> Both of double helical and triple helical DNA showed separated <sup>31</sup>P resonance signals from dT and dA strands at 10 °C, which is below melting temperature, and they were distinguishable (Figures not shown). The signals merged into one broad resonance signal upon interacting with TMAP, indicating fast chemical exchange between free DNA and DNA-TMAP complex. This meant that the interaction between TMAP and DNA regarded to be very weak.

## CONCLUSIONS

Binding of TMAP to DNA appeared to be very complex and weak. Absence of the isosbestic point of the UV absorption spectra for binding of TMAP to both of DNA duplex and triple helix meant no single binding patterns. Results from NMR, UV melting and CD experiments showed the binding site is regarded to be central six base pairs. Two positive groups of TMAP might bind to two negative phosphates on the same strand one by one, and two residual positive groups of TMAP might bind to two negative phosphates on the other strand crossing the major groove. This kind of binding mode is called as the surface-binding. So TMAP binding caused a considerable improvement in thermal stability for a double helical (dA)<sub>12</sub>·(dT)<sub>12</sub>, compared to triple helical (dT)<sub>12</sub>·(dA)<sub>12</sub>·(dT)<sub>12</sub> which the third (dT)<sub>12</sub> interfere the surface binding of TMAP in the major groove. Instead, self-stacking was dominant for TMAP binding to (dT)<sub>12</sub>·(dA)<sub>12</sub>·(dT)<sub>12</sub>. The different binding modes could explain the difference in the melting temperature between complexes of TMAP-(dT)<sub>12</sub>·(dA)<sub>12</sub> duplex and TMAP-(dT)<sub>12</sub>·(dA)<sub>12</sub>·(dT)<sub>12</sub> triple helix.

### *Acknowledgement*

This work was partly supported by CNU Research Fund in 2005.

## REFERENCES

1. R. J. Fiel, J. C. Howard, E. H. Mark, and N. Datta Gupta, *Nucleic Acids Res.*, **6**, 3093-3118 (1979).
2. Dougherty, T. J., *J. Natl. Cancer Inst.*, **90**, 889-905 (1989).
3. Villanuava A., Caggiari L., Jori G, and Milanesi C. *J. Photochem. Photobiol.*, **B 23**, 49-56 (1994) .
4. David A. Musser, Nirmalendu Datta-Gupta, and Robert J. Fiel *Biochem. Biophys. Res. Comm.* , **97**, 918-925 (1980).
5. Sashikumar Mettath, Benjamin R. Munson, and Ravindra K. Pandey, *Bioconjugate*

- Chem.*, **10**, 94-102 (1999).
6. Mark J. Carvlin and Robert J. Fiel, *Nucleic Acids Research*, **11**, 6121-6139 (1983).
  7. Luigi G. Marzilli, Debra L. Banville, Gerald Zon, and W. David Wilson, *J. Am. Chem. Soc.*, **108**, 4188-4192 (1986).
  8. Kevin Ford, Keith R. Fox, Stephan Neidle, and Michael J. Waring *Nucleic Acids Research*, **15**, 2221-2234 (1987).
  9. Nancy E. Mukundan, Gabor Pethö, Dabney W. Dixon, and Luigi G. Marzilli, *Inorg. Chem.*, **34**, 3677-3687 (1995).
  10. Young-A Lee, Jin-Ok Kim, Tae-Sub Cho, Rita Song, and Seog K. Kim, *J. Am. Chem. Soc.*, **125**, 8106-8107 (2003).
  11. Shieh, H-S, Berman, H. M., Dabrow, M., and Neidle, S., *Nucleic Acids Res.*, **8**, 85-97 (1980)